Available online at website: https://journal.bcrec.id/index.php/bcrec

Bulletin of Chemical Reaction Engineering & Catalysis, 19 (2) 2024, 318-326

Research Article

Sonochemical Assisted Synthesis of Cr-PTC Metal Organic Framework, ZnO, and Fe_3O_4 Composite and Their Photocatalytic Activity in Methylene Blue Degradation

Siti Nurbayti[1], Adawiah Adawiah[2], Uly Fitria Bale[1], Rizka Fadhilla[1], Fitri Nur Ramadhan[1], Agustino Zulys[3]*, Dede Sukandar[1], Nanda Saridewi[4], Latifah Tulhusna[5]

[1]Department of Chemistry, Faculty of Science and Technology, UIN Syarif Hidayatullah Jakarta, Jl. Ir. H. Juanda No. 95 Ciputat Tangerang Selatan 15412, Indonesia
[2]Integrated Laboratory Centre, Faculty of Science and Technology, UIN Syarif Hidayatullah Jakarta, Jl. Ir. H. Juanda No. 95 Ciputat Tangerang Selatan 15412, Indonesia
[3]Department of Chemistry, Faculty of Mathematics and Natural Sciences, University of Indonesia, Jl. Lingkar Kampus Raya, Pondok Cina, Beji, Depok, Jawa Barat 16424, Indonesia
[4]Department of Chemistry Education, Faculty of Tarbiya and Teaching Sciences, UIN Syarif Hidayatullah, Jl. Ir. H. Juanda No. 95 Ciputat Tangerang Selatan 15412, Indonesia
[5]Department of Public Health, Faculty of Health Science, UIN Syarif Hidayatullah Jakarta, Jl. Kertamukti No. 5, Ciputat, South Tangerang, Banten 15412, Indonesia

Received: 9th May 2024; Revised: 23th June 2024; Accepted: 23th June 2024
Available online: 28th June 2024; Published regularly: August 2024

Abstract

Methylene blue pollutants can be treated by photocatalytic methods using metal oxide-based semiconductor materials and metal organic framework (MOF). These two materials are often coupled into a composite to improve their physicochemical properties and catalytic activity. This research focuses on the synthesis of composites based on Cr-PTC MOF, ZnO, and Fe_3O_4 by the sonochemical method. The obtained composites were characterized and tested for catalytic activity in methylene blue pollutant degradation in an aqueous system under acidic conditions (pH = 5). Our investigation shows that the Cr-PTC@Fe_3O_4 composite possesses the lowest band gap energy of 1.86 eV and achieves the highest photocatalytic activity in methylene blue degradation at solution pH = 5, with a percent degradation of 84.36%. The sonochemical incorporation of Fe_3O_4 and Cr-PTC MOF is able to fabricate materials in a short time with better photocatalytic activity in degrading methylene blue than the single materials.

Keywords: Cr-PTC MOF; ZnO; Fe3O4; composite; methylene blue; sonochemical

How to Cite: S. Nurbayti, A. Adawiah, U. F. Bale, R. Fadhillah, F. N. Ramadhan, A. Zulys, D. Sukandar, N. Saridewi, L. Tulhusna, (2024). Sonochemical Assisted Synthesis of Cr-PTC Metal Organic Framework, ZnO, and Fe_3O_4 Composite and Their Photocatalytic Activity in Methylene Blue Degradation. *Bulletin of Chemical Reaction Engineering & Catalysis*, 19 (2), 318-326 (doi: 10.9767/bcrec.20156)

Permalink/DOI: https://doi.org/10.9767/bcrec.20156

1. Introduction

Batik industry is one of the largest contributors to wastewater containing hazardous organic dyes. Methylene blue is a very common dye used in batik manufacturing in dyeing process of leather, cotton, and tannin [1]. Methylene blue is toxic, carcinogenic, and extremely difficult to degrade naturally. The accumulation of methylene blue in water significantly reduces the solubility of oxygen and sunlight penetrating the water, resulting in a disruption of aquatic biota activity [2]. Methylene blue contaminant concentrations of more than 1 mg/L leads to aesthetic pollution and hinder the photosynthetic reactions of plants in the water [3].

Several methods can be employed in methylene blue elimination, including adsorption [4-5], flocculation [6], coagulation [7], and photocatalysis [8]. Photocatalysis is considered as

* Corresponding Author.
Email: zulys@ui.ac.id (A. Zulys)

the most effective method for removing methylene blue molecules from water since it utilizes sunlight as an energy source, generates more environmentally friendly end products (carbon dioxide and water), and applies catalysts that can be used continuously [9]. When semiconductors are exposed to light with an energy level higher than or equal to photocatalyst's band gap energy, they create free radical species that play an important role in the degradation process [10].

ZnO is one of the widely developed metal oxide-based photocatalysts used as it is cheap and has good photocatalytic activity [11]. Furthermore, plant extracts assist in the easy synthesis of ZnO through green synthesis methods. Plant extracts can act as capping and stabilizer agents because they contain phytochemical compounds that are responsible for the synthesis of metal and metal oxide nanostructures [12]. The use of pumpkin seed extract as a capping agent is reported to produce ZnO nanoparticles with a particle size of 28.0 nm with a hexagonal structure [11].

However, ZnO has a wide band gap energy of 3.37 eV, which means that it can only degrade dyes when exposed to ultraviolet light [13]. This limitation can be minimised by designing composites using visible light responsive materials, one of which is metal organic framework (MOF). Several studies have reported that the combination of ZnO and MOF can enhance their photocatalytic activity [14-17]. The research by Buasakun et al. found that the ZnO@MOF-46 (Zn) composite is better at degradation of methylene blue than ZnO, with a degradation percentage of 90.09% and 85.89%, respectively, in 180 minutes [17].

Chromium and perylene-based MOF (Cr-PTC) is a visible light-responsive MOF that is proven to be able to eliminate methylene blue pollutants in water through either adsorption or photocatalytic degradation mechanisms. Cr-PTC offer the advantages of a large surface area, being stable in aqueous solutions under acidic to neutral conditions, and having a low band gap energy that allows photocatalytic reactions to be conducted under visible light irradiation [18].

Additionally, combining the photocatalyst with Fe_3O_4 magnetite can enhance its effectiveness. Fe_3O_4 is used to prepare photocatalyst materials that are easy to separate after use. Magnetite Fe_3O_4 is the preferred choice because of its good magnetic properties, being cheap, stable at high temperatures, and being environmentally friendly [19]. According to Aghayi *et al.* the MOF/Fe_3O_4 composite has a crystal size of 34.70 nm, is recyclable, and can break down methylene blue when exposed to UV and visible light [20].

The selection of method is crucial in the synthesis process. The sonochemical method is a promising method to synthesize nano-sized particles due to the cavitation process of ultrasonic waves in liquid media. Synthesis using this method is classified as green synthesis or environmentally friendly, the production of high purity nano particles with minimal by-products, fast and easily controllable reaction periods, and high mixing efficiency [21]. Saridewi *et al.* reported ZnO-Fe_3O_4 magnetic nanocomposites made from a mass ratio of ZnO:Fe_3O_4 mass ratio of 4:1 has a particle size of 173.23 nm and provides optimal methylene blue degradation capacity under halogen lamp irradiation of 99.56 mg/g at pH = 13 [22]. On the other hand, Mahrunnisa et al. reported that Cr-PTC-HIna MOF synthesized via sonochemical method has a surface area of 92.76 m^2/g, pore volume of 0.39466 cm^3/g, and pore size of 142.738 Å and has a percent adsorption and photocatalytic methylene blue decolorization of 87.478% higher than Cr-PTC-HIna MOF synthesized via solvothermal method of 77.259% and hydrothermal of 64.959% [23].

According to literature review, research on the incorporation of ZnO, Fe_3O_4 and MOFs especially using the sonochemical method are still scarcely found. Therefore, the objective of this study was to synthesize composites based on ZnO, Cr-PTC MOF, and Fe_3O_4 using sonochemical method. The obtained composites were analysed for their physico-chemical characteristics as well as their ability to degrade methylene blue in an aqueous solution.

2. Materials and Methods

2.1 Materials

The materials used in this study include distilled water, dried pumpkin seeds (*Curcubita moschata* D.), N,N-dimethyl formamide (DMF) emsure grade P.A. (Loba Chemie PVT, LTD), peryelene-3,4,9,10-tetracarboxylic dianhydride (PTCDA) (Sigma Aldrich), technical grade ethanol (Merck), Iron(II) sulfate $FeSO_4.7H_2O$ (Merck), chromium chloride hexahydrate ($CrCl_3.6H_2O$), $FeCl_3.6H_2O$ (Merck), methylene blue (Merck), sodium hydroxide (NaOH) emsure grade (Merck), and zinc acetate dihydrate ($Zn(CH_3COO)_2.2H_2O$) (Merck).

2.2 Biosynthesis of ZnO Nanoparticles

Pumpkin seeds (*Cucurbita moschata*) were washed and dried in the sun for three days. Dried pumpkin seeds were mashed with a grinder to obtain pumpkin seed flour. 10 g of pumpkin seed flour was added to 100 mL of distilled water and heated at 100 °C in a water bath for 25 minutes. The solution was filtered with Whatman filter paper no. 41 to obtain pumpkin seed extract. Pumpkin seed extract (*Curcubita moschata* D.) of as much as 10 mL was added to 90 mL of 0.15 M

$Zn(CH_3COO)_2.2H_2O$. Next, the mixture was heated at 70 ℃ for 1 h in an aqueous bath system while stirring at 400 rpm. Then, 0.1 M NaOH was added until the mixture reached pH 8. Next, the mixture was heated while stirring to form a solid gel. The white solid gel obtained was then centrifuged at 4000 rpm at room temperature. Then, the sol-gel was rinsed using distilled water and dried for 18 h at 100 ℃. Then, the obtained solid was calcined for 4 h at 450 ℃.

2.3. Synthesis of Fe_3O_4

A total of 4 g of $FeCl_3.6H_2O$ and 2 g of $FeSO_4.7H_2O$ were dissolved in 100 mL of distilled water and stirred for 30 min. Next, 100 mL of 10% (w/w) NaOH was added to the mixture while magnetically stirred at 600 rpm for 4 h at 60 °C. Next, the black precipitate formed was filtered and rinsed with deionized water until pH 7. Finally, the black precipitate was dried for 8 h at 60 °C.

2.4. Preparation of Sodium Perylene-3,4,9,10-tetracarboxylate (Na_4PTCDA)

Perylene-3,4,9,10-tetracarboxylicdianhydride (PTCDA) (0.5 g; 1.27 mmol) was dissolved in 50 mL of distilled water, and NaOH (0.356 g; 8.9 mmol) was added. Then the mixture was stirred for 1 h at 300 rpm. Next, the greenish-red solution was filtered, and excess ethanol was added to obtain a yellow Na_4PTC precipitate. The Na_4PTC precipitate obtained was then filtered and rinsed with ethanol until it reached a neutral pH. After that, the precipitate was dried at room temperature for 24 h.

2.5. Synthesis of Composites

Cr-PTC@ZnO: $CrCl_3.6H_2O$ salt (0.266 g, 1 mmol), Na_4PTC (0.258 g, 0.5 mmol), and ZnO (0.087 g, 1 mmol) were dissolved in 30 mL of DMF solvent. Then the mixture was stirred at 300 rpm for 1 h. The mixture was then transferred into the ultrasonicator. The sonication process took 60 minutes at 25 °C with a frequency of 60 Hz and a voltage of 240 V. The precipitate formed was filtered and rinsed with hot distilled water until the filtrate was clear. The precipitate was then dried at 70 °C for 24 h.

Cr-PTC@Fe_3O_4: $CrCl_3.6H_2O$ salt (0.266 g, 1 mmol), Na_4PTC (0.258 g, 0.5 mmol), and Fe_3O_4 (0.232 g, 1 mmol) were dissolved in 30 mL of DMF. Then, the mixture was stirred at 300 rpm for 1 h and transferred into an ultrasonicator. The sonication process took 60 minutes at 25 °C with a frequency of 60 Hz and a voltage of 240 V. The precipitate formed was filtered and rinsed with hot distilled water until the filtrate was clear. The precipitate was then dried at 70 °C for 24 h.

Cr-PTC@ZnO-Fe_3O_4: $CrCl_3.6H_2O$ salt (0.266 g, 1 mmol), Na_4PTC (0.258 g, 0.5 mmol), ZnO (0.087 g, 1 mmol), and Fe_3O_4 (0.232 g, 1 mmol) were dissolved in 30 mL of DMF solvent. Then the mixture was stirred at 300 rpm for 1 h. The mixture was then transferred into an ultrasonicator. The sonication process took 60 minutes at 25 °C with a frequency of 60 Hz and a voltage of 240 V. The precipitate formed was filtered and rinsed with hot distilled water until the filtrate was clear. The precipitate was then dried at 70 °C for 24 h.

2.6. Characterizations

The diffraction pattern of the composite was analyzed using XRD (Shimadzu XRD-7000 Maxima) with monochromatic Cu-Kα radiation (λ = 1.54056 Å). The crystal size was calculated using the Debye-Scherrer equation. Functional group analysis was measured by FTIR Prestige 21 Shimadzu in the wave number range of 400–4000 cm^{-1} with a spectral resolution of 4 cm^{-1}, and KBr as a blank. Band gap energy values were measured with a Thermo-Scientific Genesys 10s UV-Vis in the 200–800 nm wavelength range, with $BaSO_4$ powder used as a blank. The band gap energy was calculated using the Kubelka-Munk equation plotted with the tauc plot.

2.7. Photocatalytic Activity Analysis

25 mg of composite was dispersed into 50 mL of 50 mg/L methylene blue and magnetically stirred at 300 rpm under 250-watt mercury lamp irradiation for 2 h. The suspension was sampled by 2 mL every 15 min and centrifuged at 6000 rpm for 10 min. The absorbance of methylene blue was measured using a UV-Vis spectrophotometer at 665 nm. The degradation efficiency (*DE, %*) was calculated using Equation (1). Methylene blue degradation testing was also carried out in dark conditions or without mercury lamp irradiation as a comparison.

$$DE = ((A_0\text{-}A_t))/A_0 \times 100\% \quad (1)$$

where, A_0 is the initial methylene blue absorbance, A_t is the absorbance of methylene blue at a specific time interval, and *DE* is the amount of methylene blue degraded.

3. Results and Discussion

3.1. Zinc Oxide (ZnO) Nanoparticle

Pumpkin seed extract (*Cucurbita moschata*) acts as a capping agent to prevent agglomeration of ZnO particles so as to obtain ZnO in nanoparticle size. Zinc acetate solution plays a role as a precursor with a concentration of 0.15 M under pH = 8 conditions because it is considered the best condition for the synthesis of ZnO nanoparticles. The pH conditions used are less than or more than 8, which may lead to

agglomeration on the particle surface so that the resulting ZnO particle size will be larger. Saridewi et al. stated that pH = 8 is a suitable condition that allows the production of ZnO nanoparticles < 35 nm [11]. Alias *et al.* reported that ZnO synthesized in acidic pH conditions has a high particle agglomeration due to the high amount of H^+ ions and low OH^- ions causing the growth of ZnO particles to be hindered, while at alkaline pH the resulting ZnO particles are nano-sized and minimal agglomeration has happened [24]. Ribut *et al.* also reported that ZnO synthesized at pH 7 is agglomerated and produces a larger ZnO particle size when compared to alkaline pH [25].

The mechanism of ZnO nanoparticle formation involves the components contained in pumpkin seed extract. Saridewi *et al.* stated that polyol compounds (phenolics and flavonoids), terpenoids, and protein compounds in pumpkin seed extract serve as stabilizing agents, templates, and capping agents [11]. The functional groups on these compounds interact with the zinc surface and encapsulate the zinc clusters, preventing aggregation between zinc clusters so that the ZnO particles formed are stable [26]. The drying process at 100 °C was carried out to remove the remaining water content. The calcination process at 450 °C contributed to the breakage of the bond between Zn and OH, which led to the formation of ZnO nanoparticles with high crystallinity.

3.2. Magnetit (Fe_3O_4)

Magnetite Fe_3O_4 is made using the co-precipitation method by reacting $FeCl_3.6H_2O$ as a source of Fe^{3+} ions and $FeSO_4.7H_2O$ as a source of Fe^{2+} (Equation (2)). The addition of NaOH serves as a precipitating agent in the formation of Fe_3O_4, which is indicated by the change in solution to black (Equation (3)) [27]. The temperature used in the synthesis of Fe_3O_4 is kept constant and does not exceed 60 ℃ to avoid excessive oxidation of Fe^{2+} ions, which contribute to the formation of Fe_2O_3, which magnetic properties are lower than those of Fe_3O_4. The black precipitate obtained is rinsed using distilled water until neutral to remove residual cations and anions in the mixture [27]. The final stage is heating, which is needed to remove the water content in the dehydration process so that Fe_3O_4 is formed as magnetite particles.

$$Fe^{2+} + 2Fe^{3+} + 8OH^- \rightarrow Fe_3O_4 + 4H_2O \quad (2)$$

$$FeSO_{4\,(l)} + 2FeCl_{3\,(l)} + 8NaOH_{(l)} \rightarrow Fe_3O_{4\,(s)} + Na_2SO_{4\,(l)} + 6NaCl_{(l)} + H_2O_{(aq)} \quad (3)$$

3.3. Composites

The stability of MOF-based composites as photocatalysis materials is highly dependent on the strength of the metal-ligand bond. The Hard Soft Acid Base (HSAB) theory states that the stability of MOFs is highly dependent on the strength of the bond between the metal and its ligand. Hard Lewis base ligands and hard Lewis acid metal ions will form strong metal ligand-ion bonds [28]. Perylene is classified as a hard Lewis base with a carboxylic functional group (COO-), while chromium metal ions (Cr^{3+}) are classified as hard Lewis acids. Reacting the two of them can produce a stable MOF.

The sonochemical method was chosen in synthesising composites as it can break large crystal aggregates into small nano-scale sizes. So that, in its application as a photocatalysis material, it can produce composite materials with a large surface area so that their photocatalytic activity will be greater. In addition, the time and energy required during synthesis are relatively short [29].

Dimethylformamide (DMF) was the solvent of choice because it can facilitate the production of MOFs with high crystallinity using carboxylate-type ligands [30]. DMF can reduce the activation energy by releasing anions towards covalently bound cations [31]. Zhang *et al.* observed that Cu-BTC could not be successfully synthesised using aqueous solvents under ultrasonic irradiation because water inhibits the formation of coordination bonds between the carboxyl groups of BTC and Cu [32]. Besides, Israr *et al.* also reported that the synthesis of Ni-BTC with DMF solvent under ultrasonic irradiation produced a MOF framework within 2 hours, but the synthesis with water or ethanol solvent under the same condition was unsuccessful [31].

The rinsing of the sonicated sediment was carried out repeatedly until the filtrate was clear, using distilled water to remove impurities trapped on the surface or pores of the composite. The drying process serves to remove the composite's water content. Reduction of the water molecules in composite leads to an increase in its pores. The composite's pore serves as the active site, facilitating the photodegradation reaction.

3.4. Functional Group

Figure 1 shows that the IR spectra of the three composites produced have slight differences compared to the IR spectrum of Cr-PTC in previous research [18]. The new peaks formed demonstrate the changes in the spectrum (Figure 1). The three composites have absorption peaks at 3500–3000 cm^{-1} which indicate the stretching vibrations of the O–H group caused by the presence of H_2O adsorbed on the surface of the three composites. The three composites have absorption peaks at 1759–1750 cm^{-1} representing asymmetric and symmetric stretching vibrations of the (C=O) carbonyl group. The absorption peaks at 1436–1351 cm^{-1} correspond to C–O functional groups, confirming the presence of carboxylic groups. The IR spectra of Cr-PTC@ZnO, Cr-PTC,

Cr-PTC@Fe_3O_4, and Cr-PTC@ZnO-Fe_3O_4 display Cr–O absorption at 673-641 cm^{-1}, corresponding to the interaction between Cr and O atoms on the carboxylic group of the perylene linker. This was also found in research by Shadmehr *et al.* which found the absorption peak of the Cr–O group at 674 cm^{-1}. The Cr-PTC@ZnO and Cr-PTC@ZnO-Fe_3O_4 composites exhibit absorption at 532 and 517 cm^{-1} suggesting the presence of Zn–O bonds, where the characteristic of these bonds is present in the fingerprint region at 550–453 cm^{-1} [33]. The Cr-PTC@Fe_3O_4 and Cr-PTC@ZnO-Fe_3O_4 composites show an absorption peak at 590 cm^{-1} which signifies the presence of a Fe–O bond in Fe_3O_4.

3.5. Diffraction Pattern

Figure 2 shows that the Cr-PTC@ZnO composite has sharp intensities at 2θ = 6.21°; 12.46°; 15.56°; 19.29°; 22.24°; and 26.92°, which are the diffraction peaks of Cr-PTC MOF [18]. ZnO diffraction peaks were also detected at 2θ = 31.74°, 34.37°, and 36.21° (JCPDS ZnO No. 01-088-0315), but with low intensity. The diffraction peaks of Cr-PTC are sharper than those of ZnO; this is due to the composition of Cr-PTC, which is higher than that of ZnO. The Cr-PTC@ZnO-Fe_3O_4 composite has sharp intensity at 2θ = 6.21°; 12.46°; 15.56°; 19.29°; 22.24°; 26.92°; 30.3°; 35.03o; 43.22°; 57.0°. Meanwhile, the Cr-PTC@Fe_3O_4 composite only shows four sharp peaks at 2θ = 30.3°, 35.03°, 43.22°, and 57.0°, which is characteristic of the Fe_3O_4 compound (JCPDS No. 85-1436). It indicates the crystallinity level of Fe_3O_4 > Cr-PTC MOF > ZnO.

3.6. Band Gap Energy

Figure 3 shows that Cr-PTC@ZnO, Cr-PTC@Fe_3O_4, and Cr-PTC@ZnO-Fe_3O_4 composites have band gap energies of 2.32 eV, 1.86 eV, and 2.34 eV, respectively. Rana *et al.* reported that ZnO nanoparticles have a band gap of 3.22 eV with maximum light absorption at the 396 nm wavelength [34]. It can be seen that when compared to ZnO, the band gap energy decreases from 3.22 eV to 2.32 and 2.34 eV for Cr-PTC@ZnO and Cr-PTC@ZnO-Fe_3O_4 (Figure 3a, 3c). Meanwhile, Abadiah *et al.* stated that the band gap energy of Fe_3O_4 was 2.22 eV. When compared with Fe_3O_4, the energy band gap for Cr-PTC@Fe_3O_4 decreased from 2.2 eV to 1.86 eV (Figure 3b). The decreasing band gap energy in the three composites is due to the organic linker perylene and chromium metal ions used in the composite synthesis being responsive to visible light [35]. The perylene linker has five aromatic rings. The number of aromatic rings causes a large number of conjugated π bonds in the ring, which contributes to the low value of band gap energy or high responsiveness to visible light. The more aromatic rings of the linker used, the lower the band gap energy.

The composite's chromium metal, on the other hand, is a transition metal with a partially filled *d* orbital. Chromium metal has a large size and atomic number. Based on the Secondary Building Unit (SBU) principle, the larger the SBU size of a metal MOF constituent, the smaller the band gap energy value. The size of the SBU is directly proportional to the size of the atomic number, or the increase in the number of electrons in the metal atom. The band gap is also smaller because Cr^{3+} metal diffuses into the lattice of ZnO and Fe_3O_4, creating a new band gap. This allows the composite to absorb energy in a wider wavelength range [36].

3.7. Photocatalytic Activity

Figure 4 shows that under dark conditions, ZnO, Fe_3O_4, Cr-PTC MOF, Cr-PTC@ZnO, Cr-PTC@Fe_3O_4, and Cr-PTC@ZnO-Fe_3O_4 composites have a methylene blue removal percent of 34.04%, 34.69%, 30.45%, 25.63%, 70.45%, and 59.71%,

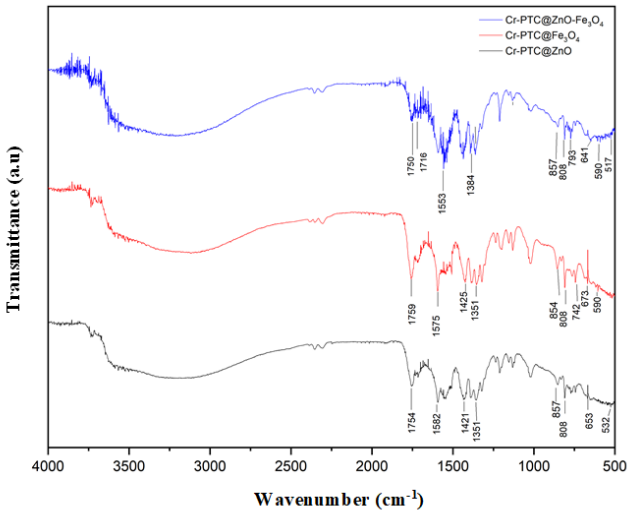

Figure 1. IR spectrum of Cr-PTC@ZnO, Cr-PTC@Fe_3O_4, and Cr-PTC@ZnO-Fe_3O_4 composite

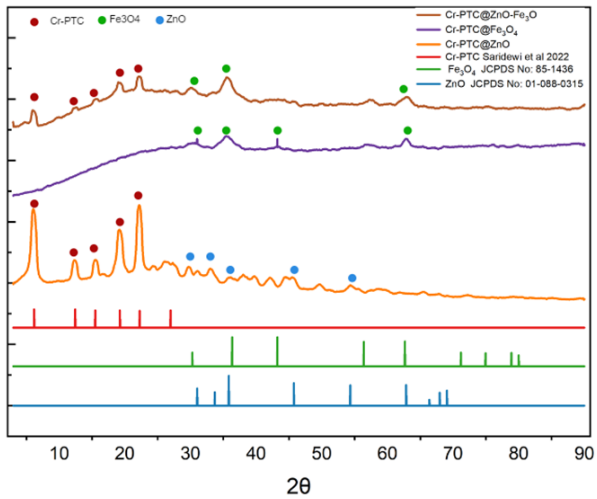

Figure 2. Diffraction pattern of Cr-PTC@ZnO, Cr-PTC@Fe_3O_4 and Cr-PTC@ZnO-Fe_3O_4

respectively. It indicates that all materials have the ability to adsorb methylene blue through an adsorption mechanism. The adsorption process between methylene blue and all materials through several interactions, including electrostatic interactions and π-π interactions. Electrostatic interaction occurs between the positive site of methylene blue, located on nitrogen atoms (N) and sulphur atoms (S), and the negative site of the MOF and three composites. For ZnO and Fe_3O_4 the electrostatic interaction can be formed between positive charge of methylene blue an negarive charge of oxygen atom. Furthermore, π-π interactions are formed between the π bond in the benzene ring in the methylene blue structure and the π bond in the benzene ring of the perylene linker contained in the Cr-PTC MOF, Cr-PTC@ZnO, Cr-PTC@Fe_3O_4, and Cr-PTC@ZnO-Fe_3O_4 composites.

In light conditions, only the Cr-PTC@Fe_3O_4 composite has photocatalytic activity in degrading methylene blue with a degradation efficiency of 84.36%. It indicates that only the Cr-PTC@Fe_3O_4 composite can degrade methylene blue through a photocatalytic degradation mechanism. The absence of catalytic activity is thought to be closely related to the electrostatic interaction between the composite and methylene blue. Methylene blue is adsorbed on the composite surface through electrostatic interaction. The stronger the interaction, the more methylene blue molecules are absorbed, and the more methylene blue can be degraded.

The pHpzc value of the material reveals the strength of the electrostatic interaction between the catalyst and methylene blue. pH_{PZC} (pH of point zero charge) is a pH value where the surface

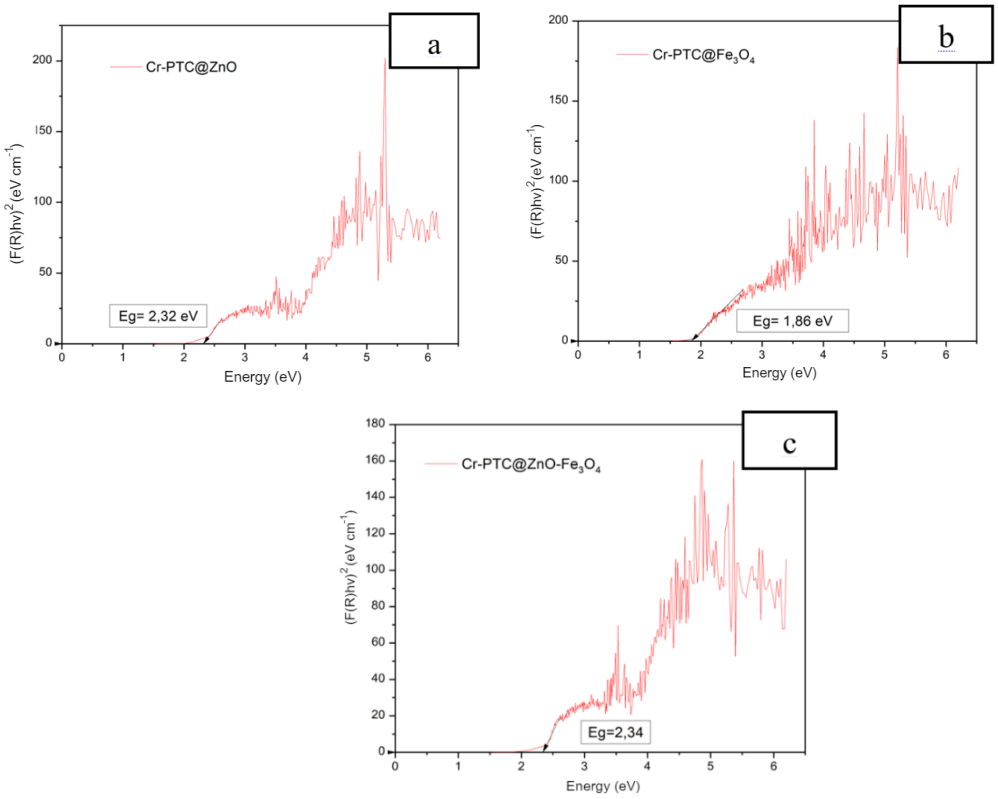

Figure 3. Band gap energy of (a) Cr-PTC@ZnO, (b) Cr-PTC@Fe_3O_4, and (c) Cr-PTC@ZnO-Fe_3O_4

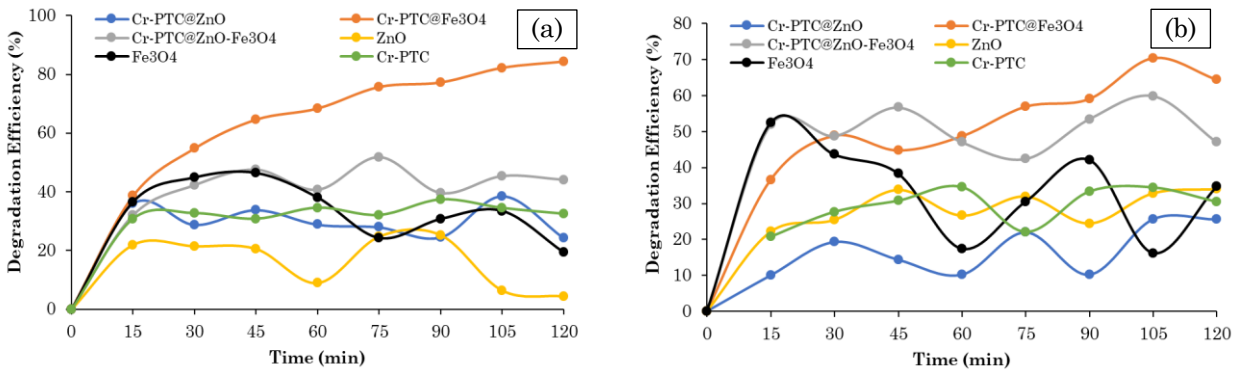

Figure 4. Degradation efficiency of methylene blue using several kinds of photocatalyst at (a) light condition and (b) dark condition

charge component of a photocatalyst material is equal to 0, or neutral. This means that there is no charge on the composite surface or that there are equal amounts of negative and positive charges. When the system pH is < pH_{PZC}, then the composite surface will be positively charged; otherwise, if the system pH is > pH_{PZC}, then the composite surface is charged.

According to Isai & Shrivastava, the pH_{PZC} value of ZnO is 8.3, while the pHpzc value of Cr-PTC MOF is 6.2. If the methylene blue solution is below the pH_{PZC} value, then ZnO and Cr-PTC MOF tend to be positively charged so they cannot interact with methylene blue which has a positive charge [37]. Meanwhile, Fe_3O_4 has a pHpzc value of 3-4 [38], and the composite formed from Fe_3O_4 and MOF Cr-PTC has a pHpzc value of 4-5. When the pH of the methylene blue solution is above the pHpzc value, which is equal to 5, the composite tends to be negatively charged, so it can interact with the positively charged methylene blue solution. The more methylene blue molecules that interact, the greater the number of methylene blue molecules that can be degraded. However, although the pHpzc value of Fe_3O_4 is below the pH of methylene blue solution, Fe_3O_4 does not show good catalytic activity in degrading methylene blue. Kalska-Szostkoa *et al.* stated that Fe_3O_4 nanoparticles undergo dissolution under acidic conditions, which is observed by a change in color in the mixture of Fe_3O_4 and acid. Dissolution occurs in the solid Fe oxide core, and ion migration into the acid solution. This is in accordance with the unstable nature of Fe in an acidic environment. This instability causes Fe_3O_4 to lose its catalytic activity [39].

Composites containing ZnO and Cr-PTC MOF compounds are less able to degrade methylene blue well under acidic pH conditions (pH = 5) because at pH = 5, the surfaces of ZnO and MOF tend to be positively charged by protonated H^+ ions. Methylene blue is positively charged cationic. The existence of these two positive charges, causes a repulsive interaction between the positive charge of MB and the catalyst which is less favorable, resulting in MB not being able to interact with the active site of the catalyst and the degradation process becomes not optimal [40]. Saridewi *et al*. reported that ZnO-Fe_3O_4 showed a decrease in photocatalytic activity at acidic pH (pH = 3-7) [22]. Saridewi *et al*. also reported that Cr-PTC MOF did not show catalytic activity in methylene blue photodegradation reactions under acidic conditions (pH = 2-5) [18].

Meanwhile, the Cr-PTC@Fe_3O_4 composite showed photocatalytic activity, where the percent degradation of methylene blue in bright conditions increased to 84.36%. The Fe_3O_4 and Cr-PTC MOF have pHpzc values below 5, so the resulting Cr-PTC@Fe_3O_4 composites tend to have similar pHpzc values. On the other hand, loading Fe_3O_4 on MOF prevents the recombination process between excited electron and electron hole pairs, which reduces the process of free radical formation and dye degradation. The presence of Fe_3O_4 also raises the number of active sites that play a role in the degradation process. In addition, Fe_3O_4 is a super magnetic material, so the resulting composite is well dispersed in methylene blue solution, so the number of composite particles that interact with methylene blue is greater. Previous research by Saridewi *et al.* provides evidence of this, reporting that the Cr-PTC MOF, without the addition of Fe_3O_4, could only degrade methylene blue by 20.74 mg/g for 180 minutes reaction time, compared to the Cr-PTC@Fe_3O_4 composite, which had a degradation capacity of 84.36 mg/g [18]. The photocatalytic degradation mechanism of methylene blue by the Cr-PTC@Fe_3O_4 composite is shown in Equations (4)–(9):

$$\text{Cr-PTC@}Fe_3O_4 + h\upsilon \rightarrow \text{Cr-PTC@}Fe_3O_4\ (e\text{-}) + \text{Cr-PTC@}Fe_3O_4\ (h^+) \quad (4)$$

$$\text{Cr-PTC@}Fe_3O_4\ (e\text{-}) + O_2 \rightarrow \bullet O_2^- \quad (5)$$

$$\text{Cr-PTC@}Fe_3O_4\ (h^+) + OH\text{-} \rightarrow OH\bullet \quad (6)$$

$$H_2O + \bullet O_2\text{-} \rightarrow 2\ OH\bullet \quad (7)$$

$$\text{Cr-PTC@}Fe_3O_4\ (h^+) + H_2O \rightarrow OH\bullet + H^+ \quad (8)$$

$$OH\bullet + MB \rightarrow \text{Degradasi} \quad (9)$$

Photon energy will expose the Cr-PTC@Fe_3O_4 photocatalyst, resulting in excited electrons in the conduction band and electron holes (h^+) in the valence band (Equation (4)). The excited electrons react with oxygen molecules attached to the photocatalyst's surface to form superoxide radical anions ($\bullet O_2^-$) (Equation (5)). These anions will react with water molecules (H_2O) adsorbed on the surface of the photocatalyst to produce hydroxide ions (OH^-), which then react with electron holes (h^+) to form OH• radicals (Equations (6)-(7)), which are strong oxidising agents for dye degradation. On the hand, h^+ reacts with water molecules (H_2O) to form hyrdoxil radical (OH•) (Equation (8)). Hyrdoxil radicals (OH•) will degrade methylene blue compounds into CO_2 and H_2O (Equation (9)) [41].

4. Conclusions

The sonochemical method can be applied to synthesise ZnO, Fe_3O_4, and Cr-PTC MOF-based composites. The Cr-PTC@Fe_3O_4 composite is characterized as the most effective photocatalyst for degrading methylene blue under acidic conditions. The Cr-PTC@Fe_3O_4 composite achieved photocatalytic degradation of methylene blue with a percent degradation rate of 84.36%.

Acknowledgments

The authors wish to thank UIN Syarif Hidayatullah Jakarta for financial support with the contract number B-304/LP2MPUSLITPEN/TL.03/2022, and Pusat Laboratorium Terpadu for facilitating this work.

CRediT Author Statement

Siti Nurbayti: Conceptualization, Methodology. Uly Fitria Bale: Formal analysis, investigation, writing original draft. Agustino Zulys: supervision. Nanda Saridewi: Supervision. Adawiah: writing, editing and reviewing. Dede Sukandar: Supervision. Rizkha Fadhilla: editing draft. Fitri Nur Ramadhan: translate draft.

References

[1] Rais, I., Nurhaeni, Ruslan, Pusptasari, D. J. (2019). Biosorben kitosan cangkang keong sawah terhadap penyerapan zat warna methylene blue. *Kovalen: Jurnal Riset Kimia*, 5 (2), 214–221. DOI: 10.22487/kovalen.2019.v5.i2.12826.

[2] Khan, I., Saeed, K., Zekker, I., Zhang, B., Hendi, A. H., Ahmad, A., Ahmad, S., Zada, N., Ahmad, H., Shah, L. A., Shah, T., Khan, I. (2022). Review on methylene blue: its properties, uses, toxicity and photodegradation. *Water (Basel)*, 14 (2), 242. DOI: 10.3390/w14020242.

[3] Aliah, H., Karlina, Y. (2015). Semikonduktor TiO_2 sebagai material fotokatalis berulang. *Jurnal ISTEK*, 9(1), 185–203.

[4] Nurhasni, N., Mar'af, R., Hendrawati, H. (2018). Pemanfaatan kulit kacang tanah (Arachis hipogaea L.) sebagai adsorben zat warna metilen biru. *Jurnal Kimia Valensi*, 4 (2), 156–167. DOI: 10.15408/jkv.v4i2.8895.

[5] Nurhasni, N., Harahap, S., Fathoni, A., Hendrawati, H. (2021). Synthesis of adsorbent from bagasse for methylene blue adsorption. *Jurnal Kimia Valensi*, 7 (2), 188–195. DOI: 10.15408/jkv.v7i2.20916.

[6] Rahmawati, L., Azis, M.M., Rochmadi, R. (2021). Methylene blue removal from waste water using sodium lignosulfonate and polyaluminium chloride: Optimization with RSM. *AIP Conference Proceedings*, 020-035. DOI: 10.1063/5.0052016.

[7] Mahecha, F.C., Parra, D.C., Sandoval, J.A., Mayoraga, M.A., Ortiz, S.A. (2021). Removal of cationic dyes utilizing natural coffee pulp coagulantns. *Chem. Eng. Trans.*, 87. 487–492. DOI: 10.3303/CET2187082.

[8] Farouq, R. (2022). Coupling adsorption-photocatalytic degradation of methylene blue and maxilon red. *J. Fluoresc.*, 32 (4), 1381–1388. DOI: 10.1007/s10895-022-02934-1.

[9] Aisien, F.A., Amenaghawon, N.A., Otuorimuo, U.O. (2014). Decolourisation of methylene blue in aqueous solution using locally sourced photocatalysts via UV irradiation photocatalytic degradation. *J. Chem.*, 2(4), 320–329.

[10] Barjasteh-Moghaddam, M., Habibi-Yangjeh, A. (2011). Effect of operational parameters on photodegradation of methylene blue on ZnS nanoparticles prepared in presence of an ionic liquid as a highly efficient photocatalyst. *Journal of the Iranian Chemical Society*, 8(S1). S169–S175. DOI: 10.1007/BF03254294.

[11] Saridewi, N., Firdaus, D.A., Aziz, I., Kumila, B.N., Dasumiati, D. (2021). Biosynthesis of ZnO nanoparticles using pumpkin peel extract (Cucurbita moschata) and its applications as semiconductor in dye sensitized solar cell (DSSC). *Jurnal Kimia Valensi*. 7(2), 100–107. DOI: 10.15408/jkv.v7i2.21046.

[12] Ishak, N.A.I.Md., Kamarudin, S.K. Timmiati, S.N. (2019). Green synthesis of metal and metal oxide nanoparticles via plant extracts: an overview. *Mater. Res. Express*, 6(11). DOI: 10.1088/2053-1591/ab4458.

[13] Bachvarova-Nedelcheva, A., Iordanova, R., Stoyanova, A., Gegova, R., Dimitriev, Y., Loukanov, A. (2013). Photocatalytic properties of ZnO/TiO_2 powders obtained via combustion gel method. *Open Chem*. 11(3). 364–370. DOI: 10.2478/s11532-012-0167-2.

[14] Roy, S., Darabdhara, J. Ahmaruzzaman, M. (2013). ZnO-based Cu metal–organic framework (MOF) nanocomposite for boosting and tuning the photocatalytic degradation performance. *Environ. Sci. Pollut. Res*., 30, 95673–95691. DOI: 10.1007/s11356-023-29105-4

[15] Li, K., de Miérand, Y.R., Jin, X., Yi, J., Guo, J. (2020). Metal Oxide (ZnO and TiO2) and Fe-based Metal–Organic-Framework nanoparticles on 3D-printed fractal polymer surfaces for photocatalytic degradation of organic pollutants. *ACS Applied Nano Materials*, 3(3), 2830-2845. DOI: 10.1021/acsanm.0c00096.

[16] Teng, D., Zhang, J., Luo, X., Jing, F., Wang, H., Chen, J., Yang, C., Zang, S., Zhou, Y. (2021). Remarkably enhanced photodegradation of organic pollutants by NH_2-UiO-66/ZnO composite under visible-light irradiation. *Journal of Renewable Material*. DOI: 10.32604/jrm.2022.019209.

[17] Buasakun, J., Srilaoong, P., Rattanakam, R., Duangthongyou, T. (2021). Synthesis of heterostructure of ZnO@MOF-46(Zn) to improve the photocatalytic performance in methylene blue degradation. *Crystals (Basel)*, 11(11), 1379. DOI: 10.3390/cryst11111379.

[18] Saridewi, N., Azhar, F.M., Abdillah, P.A., Zulys, A., Nurbayti, S., tulhusna, L., Adawiah, A. (2022). Synthesize metal-organic frameworks from chromium metal ions and ptcda ligands for methylene blue photodegradation. *RASAYAN Journal of Chemistry*, 15(04), 2544–2550. DOI: 10.31788/RJC.2022.1547046.

[19] Saffari, J., Mir, N., Ghanbari, D., Khandan-Barani, K., Hassanabadi, A., Hosseini-Tabatabaei, M.R. (2015). Sonochemical synthesis of Fe_3O_4/ZnO magnetic nanocomposites and their application in photo-catalytic degradation of various organic dyes. *Journal of Materials Science: Materials in Electronics*, 26 (12), 9591–9599. DOI: 10.1007/s10854-015-3622-y.

[20] Aghayi-Anaraki, M., Safarifard, V. (2020). Fe_3O_4@MOF magnetic nanocomposites: synthesis and applications. *Eur. J. Inorg. Chem.*, 2020 (20), 1916–1937. DOI: 10.1002/ejic.202000012.

[21] Butova, V.V., Soldatov, M.A., Guda, A.A., Lomachenko, K.A., Lamberti, C. (2016). Metal-organic frameworks: structure, properties, methods of synthesis and characterization. *Russian Chemical Reviews*, 85 (3), 280–307. DOI: 10.1070/RCR4554.

[22] Saridewi, N., Komala, S., Zulys, A., Nurbayti, S., Tulhusna, L., Adawiah, A. (2022). Synthesis of ZnO-Fe_3O_4 Magnetic Nanocomposites through Sonochemical Methods for Methylene Blue Degradation. *Bulletin of Chemical Reaction Engineering & Catalysis*, 17 (3), 650-660. DOI: 10.9767/bcrec.17.3.15492.650-660.

[23] Mahrunnisa, N., Adawiah, A., Aziz, I., Zulys, A. (2023). Green Synthesis of Cr-PTC-HIna Metal Organic Frameworks (MOFs) and Its Application in Methylene Blue Photocatalytic Degradation. *Bulletin of Chemical Reaction Engineering & Catalysis*, 18 (3), 362-374. DOI: 10.9767/bcrec.18885.

[24] Alias, S.S., Ismail, A.B., Mohamad, A.A. (2010). Effect of pH on ZnO nanoparticle properties synthesized by sol–gel centrifugation. *J. Alloys Compd.*, 499 (2), 231–237. DOI: 10.1016/j.jallcom.2010.03.174.

[25] Ribut, S.H., Abdullah, C.A.C., Mustafa, M., Yusoff, M.Z.M., Azman, S.N.A. (2018). Influence of pH variations on zinc oxide nanoparticles and their antibacterial activity. *Mater. Res. Express*, 6(2), 025016. DOI: 10.1088/2053-1591/aaecbc.

[26] Tournebize, J., Boudier, A., Joubert, O., Eidi, H., Bartosz, G., Maincent, P., Leroy, P., Sapin-Minet, A. (2012). Impact of gold nanoparticle coating on redox homeostasis. *Int. J. Pharm.*, 438 (1–2), 107–116. DOI: 10.1016/j.ijpharm.2012.07.026.

[27] Agnestisia, R. (2017). Synthesis & characterization of magnetit (Fe_3O_4) and its applications as adsorbent methylene blue. *Jurnal Sains dan Terapan Kimia*, 11(2), 61. DOI: 10.20527/jstk.v11i2.4039.

[28] Wen, Y., Zhang, P., Sharma, V.K., Ma, X., Zhou, H.C. (2021). Metal-organic frameworks for environmental applications. *Cell Rep. Phys. Sci.*, 2 (2), 100348. DOI: 10.1016/j.xcrp.2021.100348.

[29] Mahreni, M., Ristianingsih, Y. (2020). A review on metal-organic framework (MOF): synthesis and solid catalyst applications. LPPM UPN "Veteran" Yogyakarta Conference Series Proceeding on Engineering and Science Series (ESS), pp. 638–645.

[30] Noro, S. (2013). Metal–Organic Frameworks in Comprehensive Inorganic Chemistry II, Second Edition. Amsterdam: Elsevier.

[31] Israr, F., Chun, D., Kim, Y., Kim, D.K. (2016). High yield synthesis of Ni-BTC metal–organic framework with ultrasonic irradiation: Role of polar aprotic DMF solvent. *Ultrason. Sonochem.*, 31, 93–101. DOI: 10.1016/j.ultsonch.2015.12.007.

[32] Zhang, B., Zhang, J., Liu, C., Sang, X., Peng, L., Ma, X., Wu, T., Hana, B., Yang, G. (2015). Solvent determines the formation and properties of metal–organic frameworks. *RSC Adv.*, 5(47), 37691–37696. DOI: 10.1039/C5RA02440D.

[33] Shadmehr, J., Zeinali, S., Tohidi, M. (2019). Synthesis of a chromium terephthalate metal organic framework and use as nanoporous adsorbent for removal of diazinon organophosphorus insecticide from aqueous media. *J. Dispers. Sci. Technol.*, 40(10), 1423–1440. DOI: 10.1080/01932691.2018.1516149.

[34] Rana, N., Chand, S., Gathania, A.K. (2016). Green synthesis of zinc oxide nano-sized spherical particles using Terminalia chebula fruits extract for their photocatalytic applications. *Int. Nano Lett.*, 6(2), 91–98. DOI: 10.1007/s40089-015-0171-6.

[35] Abadiah, N.M., Yuliantika, D., Hariyanto, Y.A., Saputro, R.E., Masruroh, Taufiq, A., Soontaranoon, S. (2019). Nanostructure, band gap, and antibacterial activity of spinel Fe_2MO_4/OO magnetic fluids. *IOP Conf. Ser. Earth Environ. Sci.*, 276(1), 012064. DOI: 10.1088/1755-1315/276/1/012064.

[36] Hassan, M.M., Khan, W., Azam, A., Naqvi, A.H. (2015). Influence of Cr incorporation on structural, dielectric and optical properties of ZnO nanoparticles. *Journal of Industrial and Engineering Chemistry*, 21, 283–291. DOI: 10.1016/j.jiec.2014.01.047.

[37] Isai, K.A., Shrivastava, V.S. (2019). Photocatalytic degradation of methylene blue using ZnO and 2%Fe–ZnO semiconductor nanomaterials synthesized by sol–gel method: a comparative study. *SN Appl. Sci.*, 1(10), 1247. DOI: 10.1007/s42452-019-1279-5.

[38] Zhang, J., Lin, S., Han, M., Su, Q., Xia, L., Hui, Z. (2020). Adsorption Properties of magnetic magnetite nanoparticle for coexistent Cr(VI) and Cu(II) in mixed solution. *Water (Basel)*, 12(2), 446. DOI: 10.3390/w12020446.

[39] Kalska-Szostkoa, B., Wykowskaa, U., Piekut, K., Satuła, D. (2014). Stability of Fe_3O_4 nanoparticles in various model solutions. *Colloids and Surfaces A: Physicochemical and Engineering Aspects*, 450 (2014), 15-24. DOI: 10.1016/j.colsurfa.2014.03.002.

[40] Kumar, P., Pandey, P.C. (2015). Consequence of cobalt incorporation on structural and optical properties of transparent nano-crystalline ZnO thin film. *Journal of International Academy of Physical Sciences*, 20(3), 203–214.

[41] Cheng, X., Yu, X., Xing, Z. (2012). Characterization and mechanism analysis of N doped TiO_2 with visible light response and its enhanced visible activity. *Appl. Surf. Sci.*, 258(7), 3244–3248. DOI: 10.1016/j.apsusc.2011.11.072.